

Supporting Information for

***In situ* imaging the dynamics of sodium metal deposition and stripping**

Lin Geng, Chao Zhao, Jitong Yan, Chengrui Fu, Xuedong Zhang, Jingming Yao,
Haiming Sun, Yong Su, Qiunan Liu, Liqiang Zhang*, Yongfu Tang*, Feng Ding*,
Jianyu Huang*

Corresponding Author

**To whom correspondence should be addressed. E-mail: liqiangzhang85@163.com;
tangyongfu@ysu.edu.cn; f.ding@unist.ac.kr; jyhuang8@hotmail.com*

Table of Contents

Supplementary Movies S1-S12 Captions

Supplementary Figures S1-S18

Supplementary Table S1

Supplementary Movies

Description of Movie S1

An in situ TEM movie showing the deposition of Na crystal in 1 mbar CO₂ ambient (**Fig. S1d-g**). The Na crystal grows at the MWCNT/Na₂CO₃/CO₂ triple point via electrochemical plating. The movie was recorded at 5 frames/second in TEM bright field mode, and played at 35× speed.

Description of Movie S2

An in situ TEM movie showing the deposition of Na crystal in 1 mbar CO₂ ambient (**Fig. 1a-f**). The Na crystal grows directly along the MWCNT via electrochemical plating. The movie was recorded at 5 frames/second in TEM bright field mode, and played at 35× speed.

Description of Movie S3

An in situ TEM movie showing the deposition of Na crystal in 1 mbar CO₂ ambient (**Fig. S6a-f**). The Na crystal grows directly along the MWCNT via electrochemical plating. The movie was recorded at 5 frames/second in TEM bright field mode, and played at 75× speed.

Description of Movie S4

An in situ TEM movie showing the deposition of Na crystal in 1 mbar CO₂ ambient (**Fig. S7a-f**). The Na crystal grows directly along the MWCNT via electrochemical plating. The movie was recorded at 5 frames/second in TEM bright field mode, and played at 35× speed.

Description of Movie S5

An in situ ADF movie showing the stripping of the as grown Na crystal in 1 mbar CO₂ ambient (**Fig. 1m-q**). The movie was recorded at 5 frames/second, and is played at 360× speed.

Description of Movie S6

An in situ TEM movie showing the deposition of Na crystal in 1 mbar CO₂ ambient (**Fig. 2a-c**). The Na crystal grows directly along the MWCNT via electrochemical plating. The movie was recorded at 5 frames/second in TEM bright field mode, and played at 35× speed.

Description of Movie S7

An in situ ADF movie showing the stripping of the as grown Na crystal in 1 mbar CO₂ ambient (**Fig. 2g-k**). The movie was recorded at 5 frames/second, and is played at 150 × speed.

Description of Movie S8

An in situ ADF movie showing the stripping of the as grown Na crystal in 1 mbar CO₂ ambient (**Fig. S10i-p**). The movie was recorded at 5 frames/second, and is played at 140 × speed.

Description of Movie S9

An in situ TEM movie showing the deposition of Na crystal in 1 mbar CO₂ ambient (**Fig. 3**). The Na crystal grows directly along the MWCNT via electrochemical plating. The movie was recorded at 5 frames/second in TEM bright field mode, and played at 60× speed.

Description of Movie S10

An in situ ADF movie showing the stripping of the as grown Na crystal in 1 mbar CO₂ ambient (**Fig. 3**). The movie was recorded at 5 frames/second, and is played at 380× speed.

Description of Movie S11

An in situ ADF movie showing the stripping of the as grown Na crystal in 1 mbar CO₂ ambient (**Fig. S12m-x**). The movie was recorded at 5 frames/second, and is played at 220 × speed.

Description of Movie S12

An in situ ADF movie showing the stripping of the as grown Na crystal in 1 mbar CO₂ ambient (**Fig. S15a-l**). The movie was recorded at 5 frames/second, and is played at 130 × speed.

Supplementary Figures

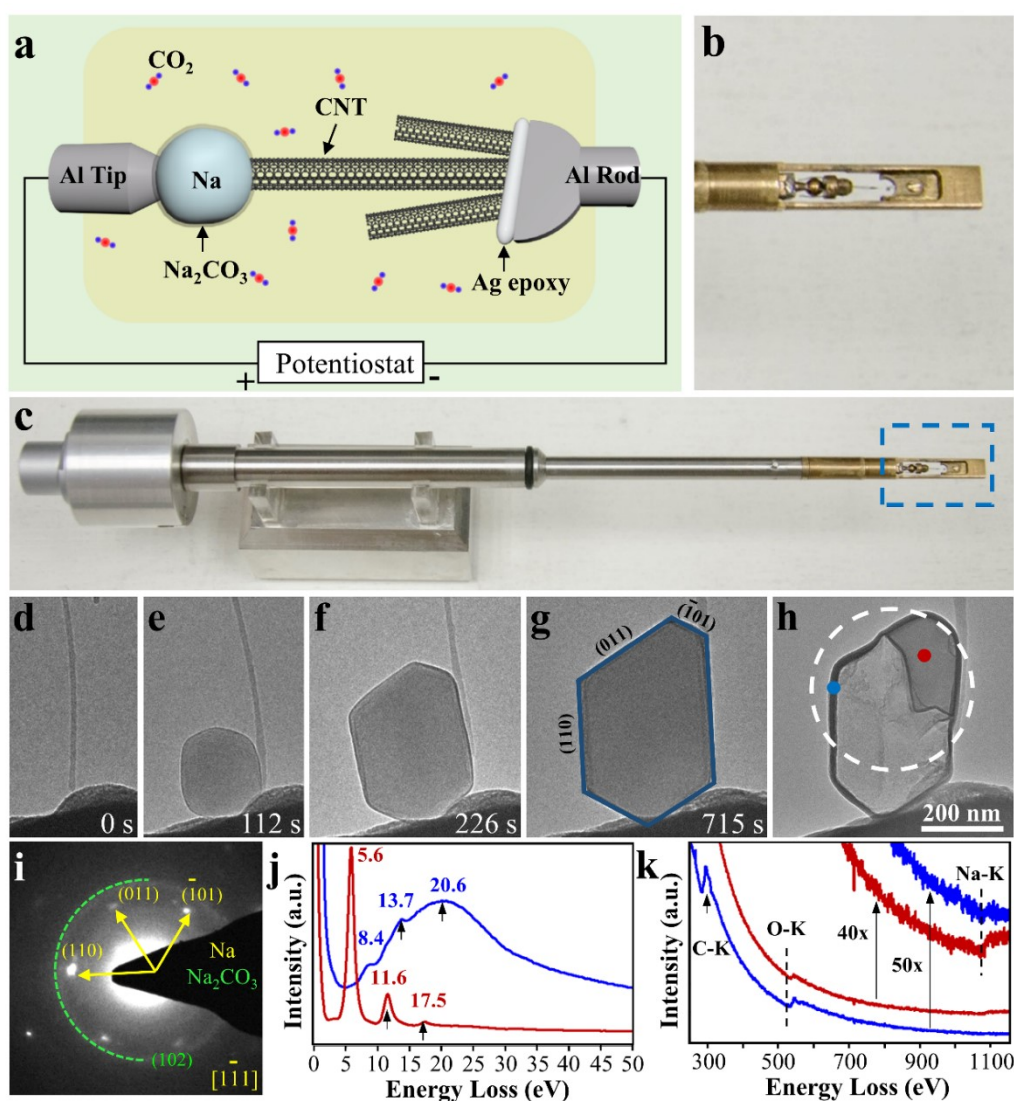


Fig. S1 *In situ* plating of Na and TEM characterization. (a) Schematic of the electrochemical setup for Na plating and stripping in ETEM. (b-c) The TEM-STM platform. (d-g) Time lapse TEM images showing the growth of a Na crystal via electrochemical plating. (h) Residual Na with Na₂CO₃ shell after stripping. (i) An EDP of the Na crystal corresponding to (h), showing diffraction spots superimposed on diffraction rings which are indexed as the [111] zone axis of Na and Na₂CO₃, respectively. A thin layer of Na₂CO₃ was formed on the surface of the Na metal. Low-loss (j) and core-loss (k) EELS of the Na crystal (red plot) and Na₂CO₃ shell (blue plot), respectively.

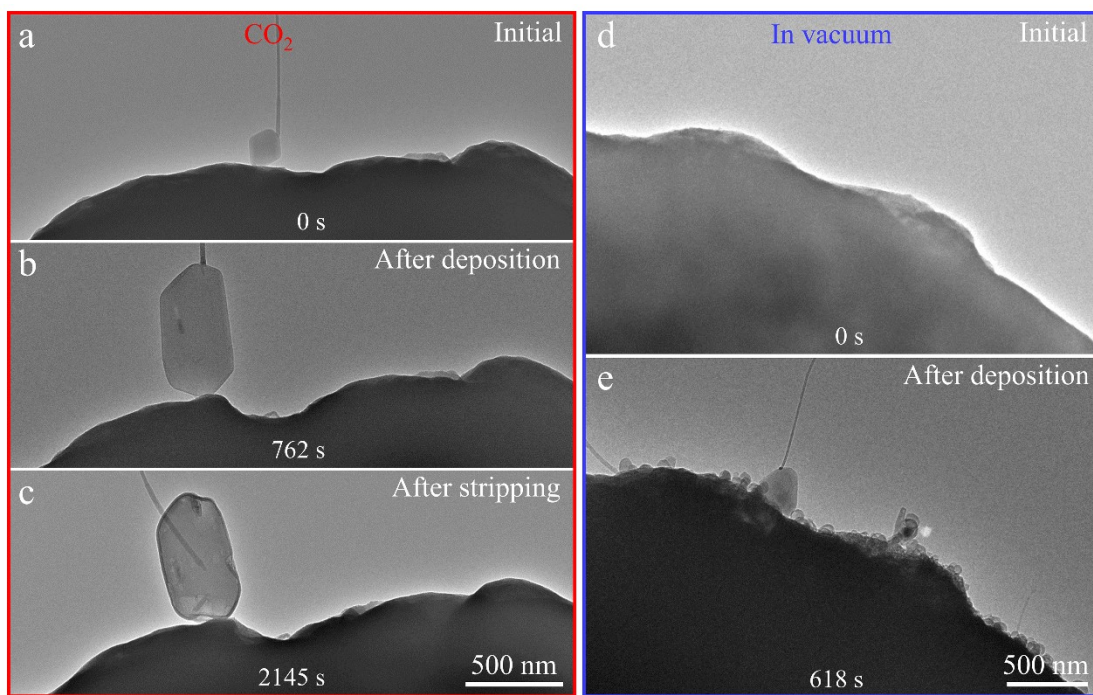


Fig. S2 Time lapse TEM images showing bulk Na surface morphology evolution during deposition and stripping. (a-c) Bulk Na surface morphology evolution in CO₂ atmosphere. (d-e) Bulk Na surface morphology evolution in vacuum.

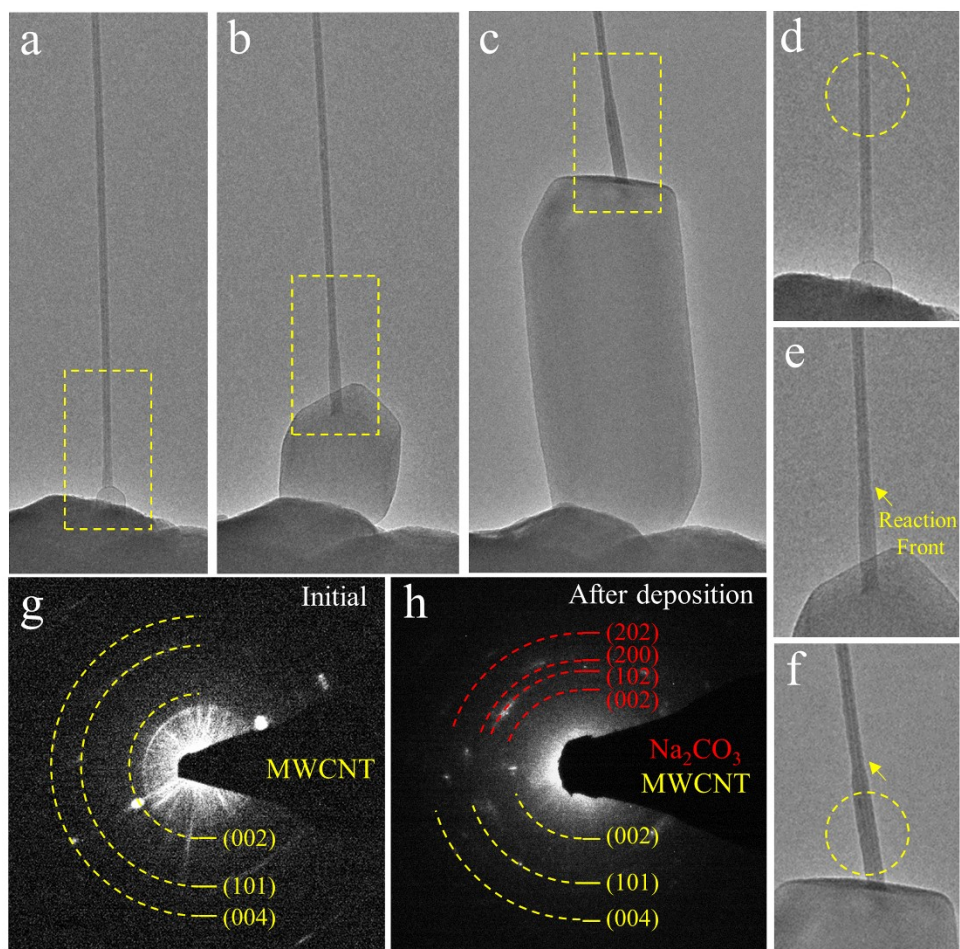


Fig. S3 Sequential TEM images of MWCNT during Na deposition with corresponding EDPs. (a-c) TEM images of the MWCNT during Na deposition, (d-f) Magnified view of the MWCNT corresponding to the yellow-boxed regions in (a-c), respectively. (g) EDP of the original MWCNT acquired from the circled region in (d). (h) EDP of the MWCNT after sodiation acquired from the circled region in (f).

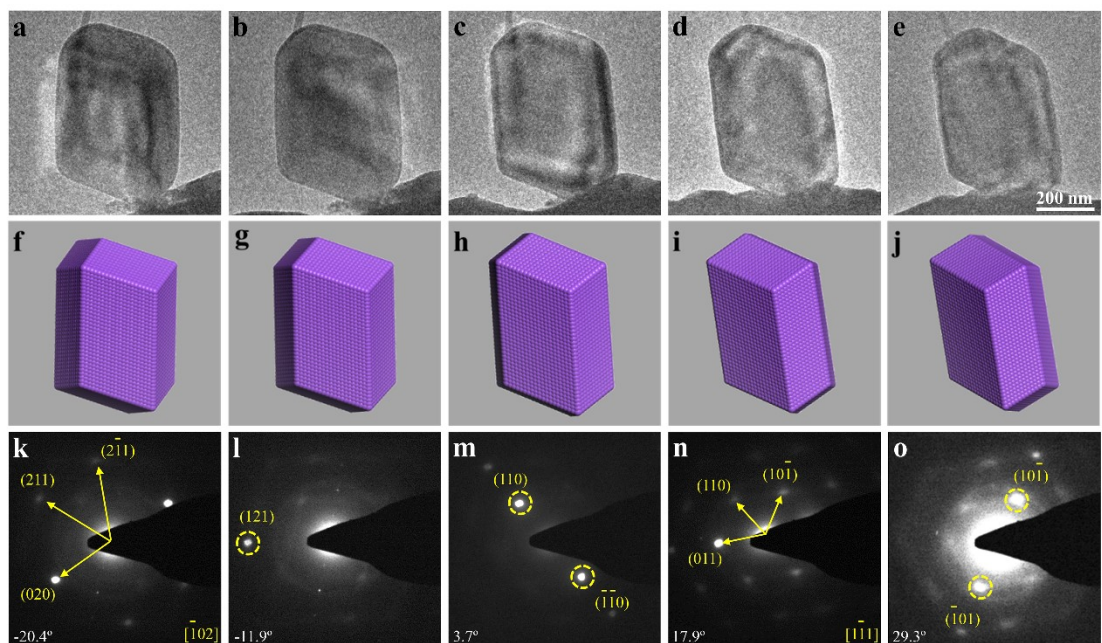


Fig. S4 Serial titling views of the Na polyhedron. (a-e) Sequential tilting of the as grown Na polyhedron from -20.4° to 29.3° . (f-j) The corresponding atomic models. (k-o) The corresponding EDPs.

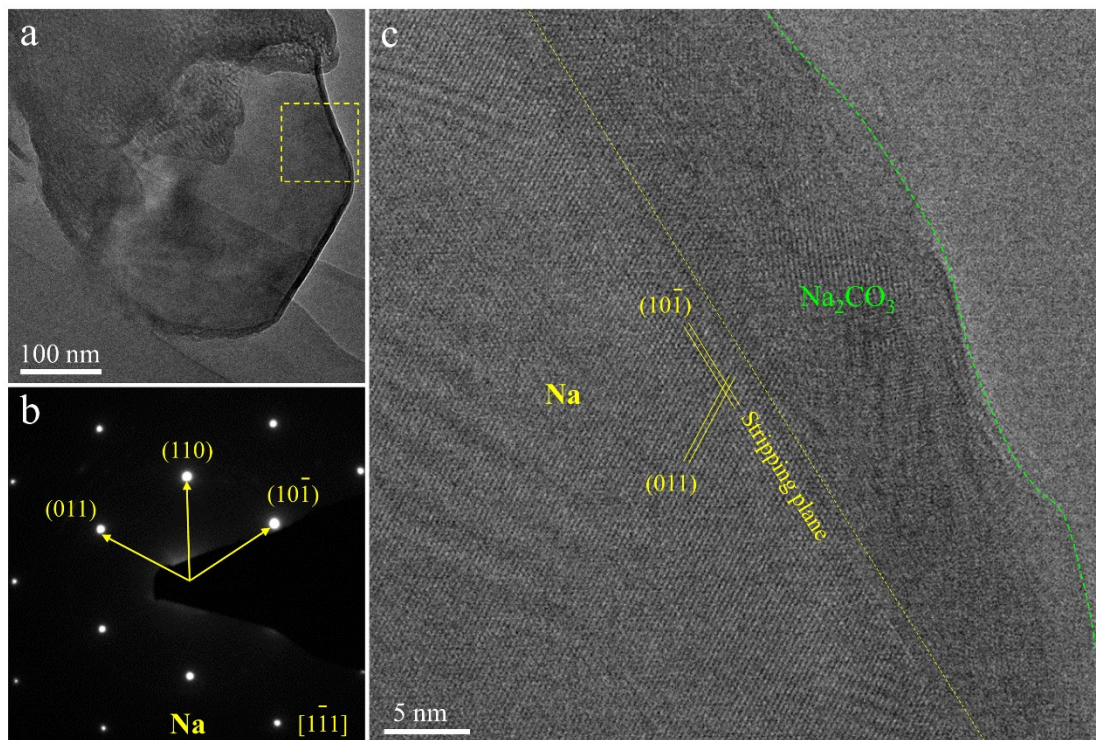


Fig. S5 HRTEM characterization of the Na dendrites. (a) Low magnification TEM image of a Na polyhedron. (b) An EDP of the polyhedron, which can be indexed as $[1\bar{1}1]$ zone axis of body-centered-cubic (bcc) Na. (c) HRTEM image corresponding to the yellow boxed region in (a).

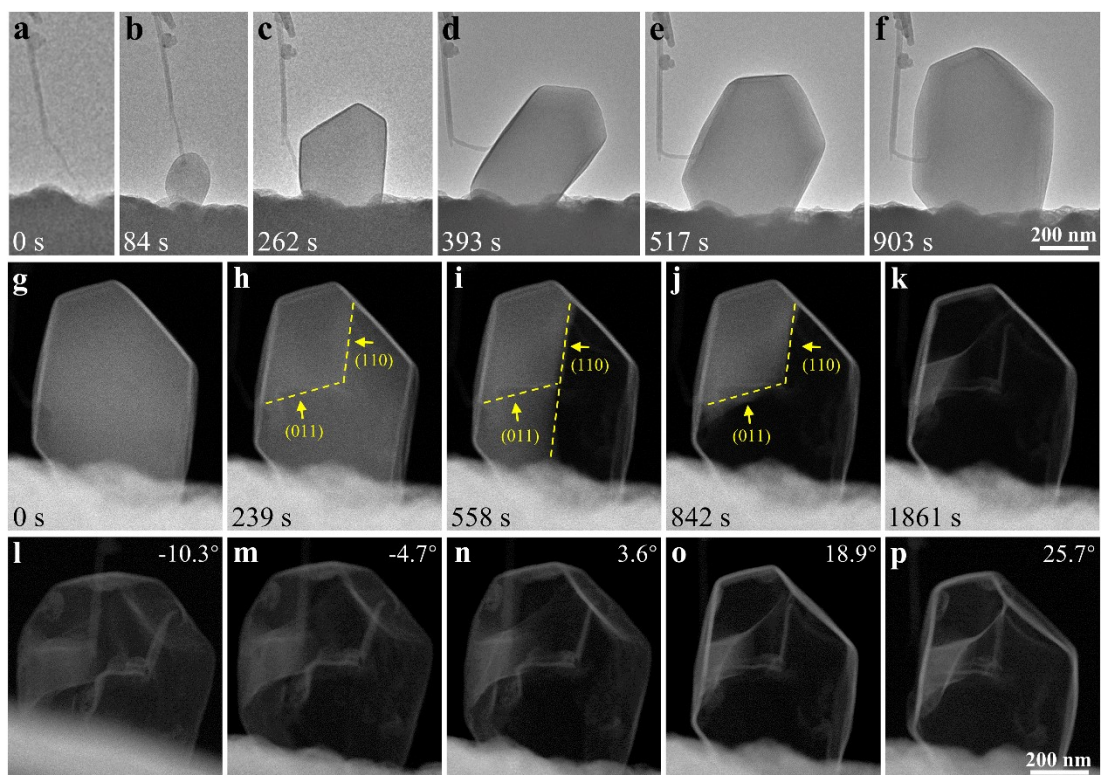


Fig. S6 *In situ* deposition and stripping of Na crystal. (a-f) Time lapse TEM images of a Na polyhedron deposition. (g-k) Time lapse ADF images of a Na polyhedron stripping. (l-p) Serial tilting images of a Na polyhedron from -10.3° to 25.7° after stripping.

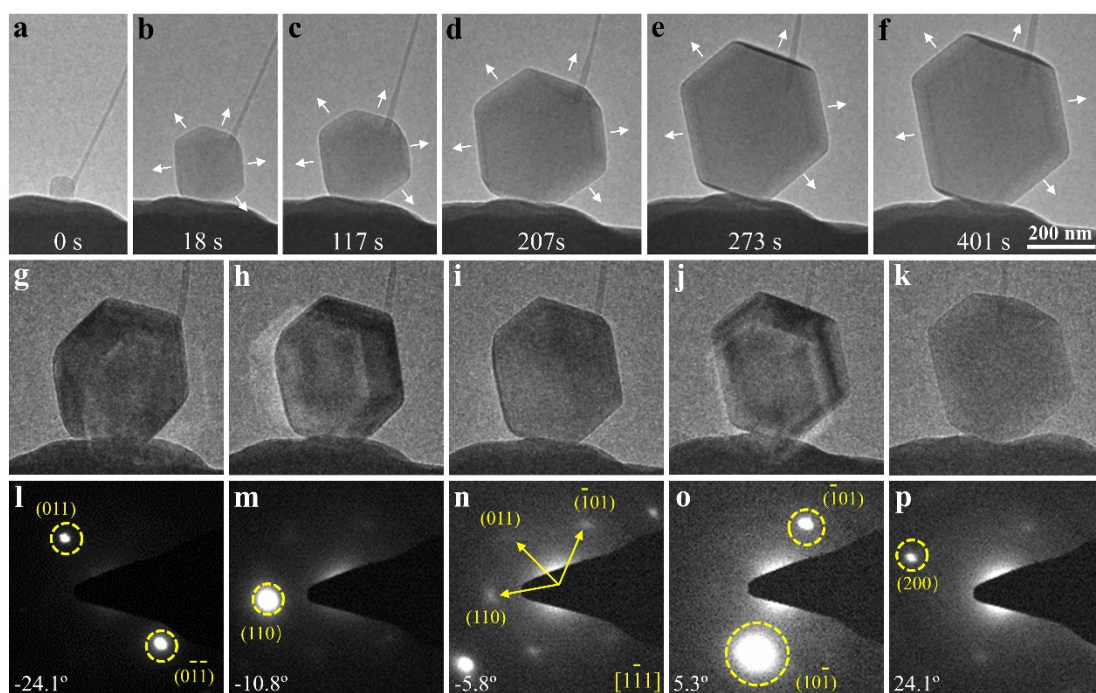


Fig. S7 Time lapse TEM images of Na crystal deposition. (a-b) Upon applying a negative potential to the MWCNT against the Na anode, a polyhedron emerged at the MWCNT, Na_2CO_3 and CO_2 triple point. (c-f) Growth of a Na polyhedron during electrochemical plating and this process appeared to be isotropic. (g-k) Serial tilting images the as grown Na polyhedron from -24.1° to 24.1° . (l-p) EDPs of the Na crystal corresponding to (g-k).

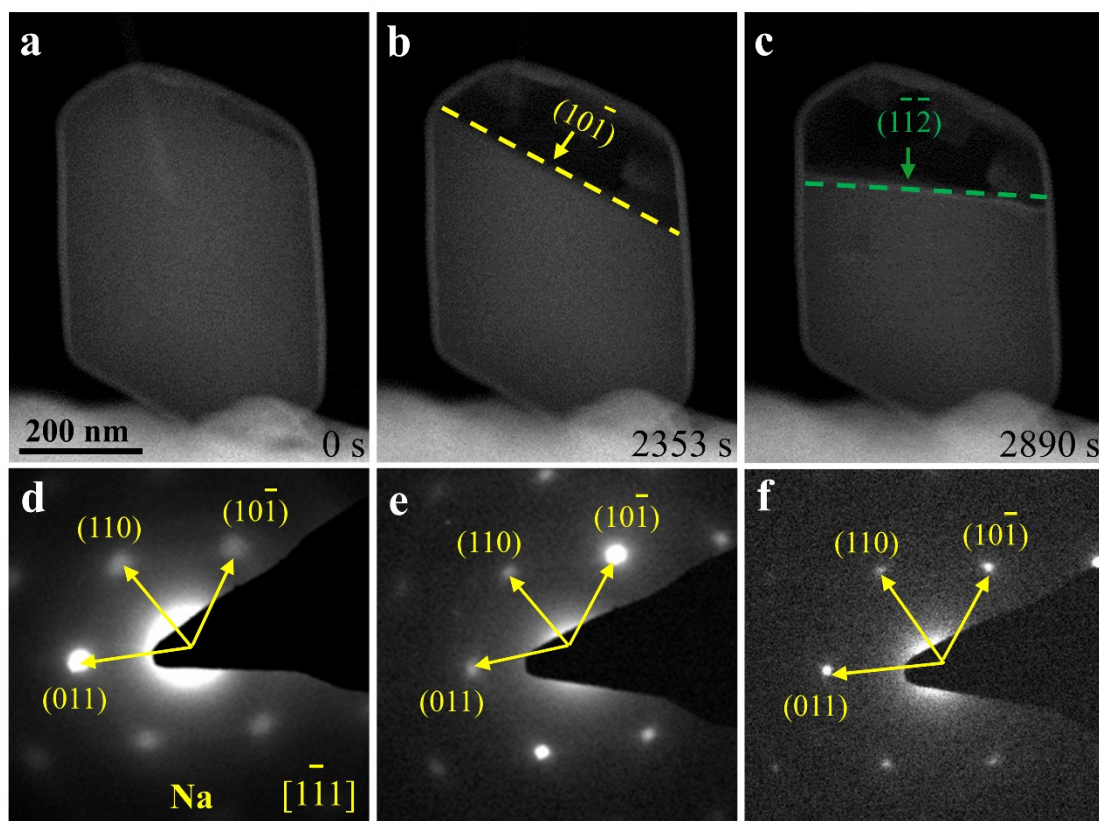


Fig. S8 Sequential ADF images of Na stripping with corresponding EDPs. (a-c) ADF images of the original, intermediate and final state during stripping process, respectively. (d-f) EDPs of the Na polyhedron corresponding to (a-c), respectively.

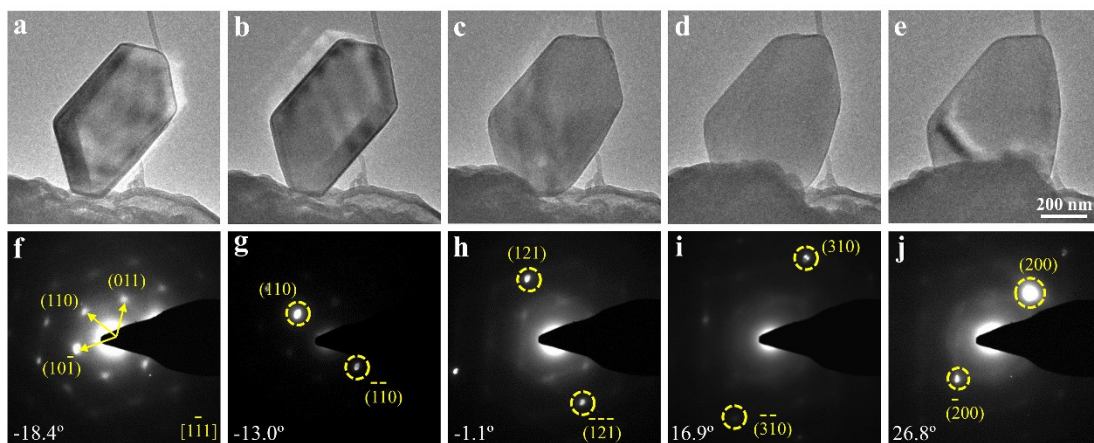


Fig. S9 Serial tilting views of a Na polyhedron. (a-e) Tilting of the as grown Na polyhedron from -18.4° to 26.8° . (f-j) The corresponding EDPs.

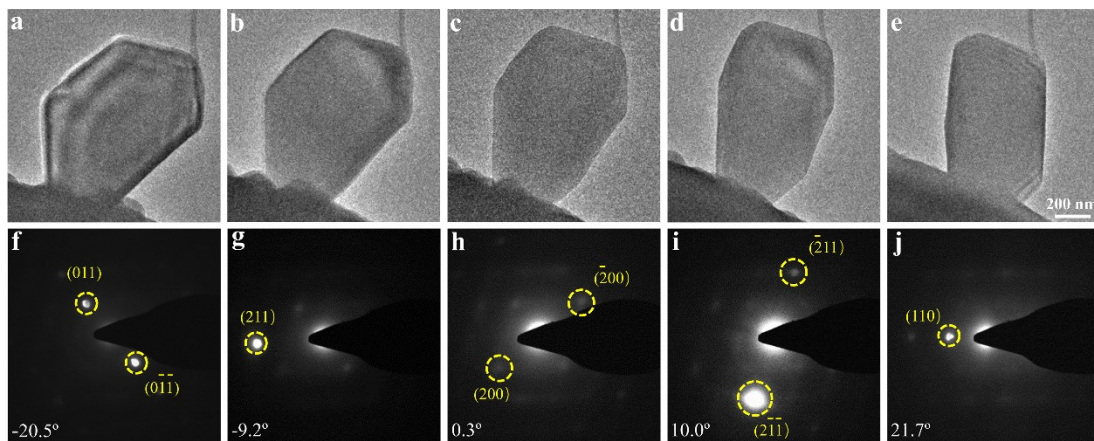


Fig. S11 Serial tilting views of a Na polyhedron. (a-e) Tilting of the as grown Na polyhedron from -20.5° to 21.7° . (f-j) The corresponding EDPs.

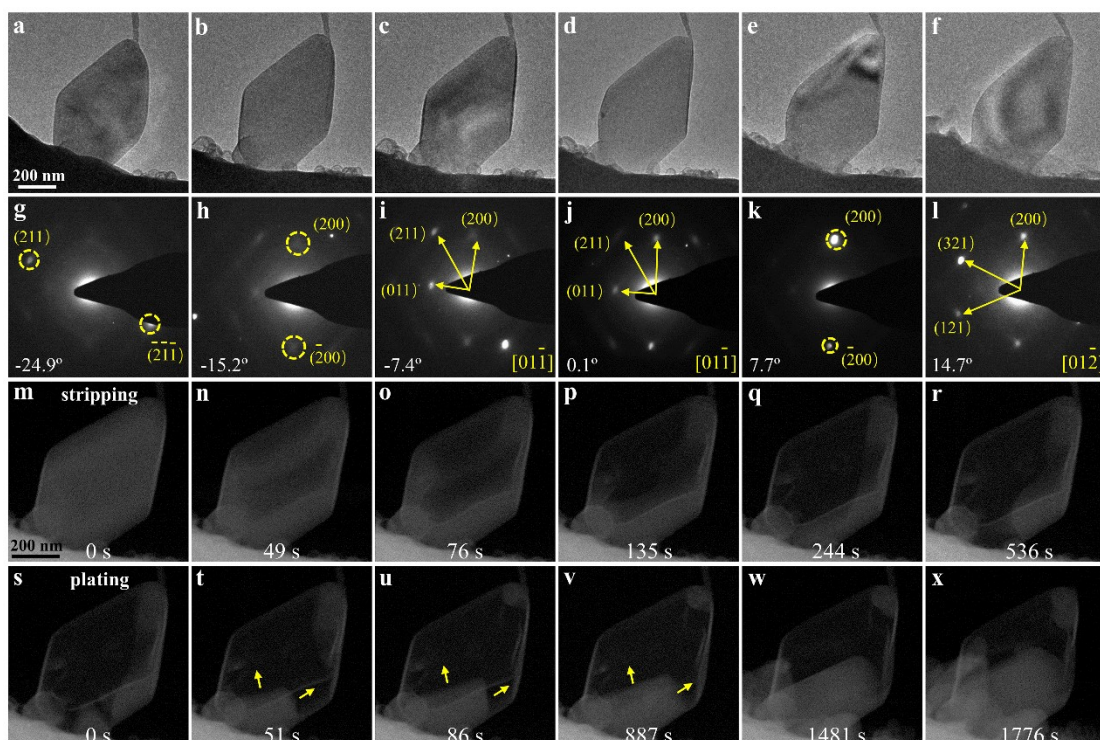


Fig. S12 Time lapse ADF images of a reversible Na deposition at the MWCNT/Na₂CO₃ contact during plating/stripping cycles. (a-f) Tilting from -24.9° to 14.7° of a Na polyhedron. (g-l) EDPs of the Na crystal corresponding to (a-f). (m-x) ADF images of the morphology evolution of the stripping and plating process. The viewing direction is $[01\bar{1}]$. Different from the $[1\bar{1}1]$ zone axis, the stripping planes are not well defined, but there exists facet during plating (t-w).

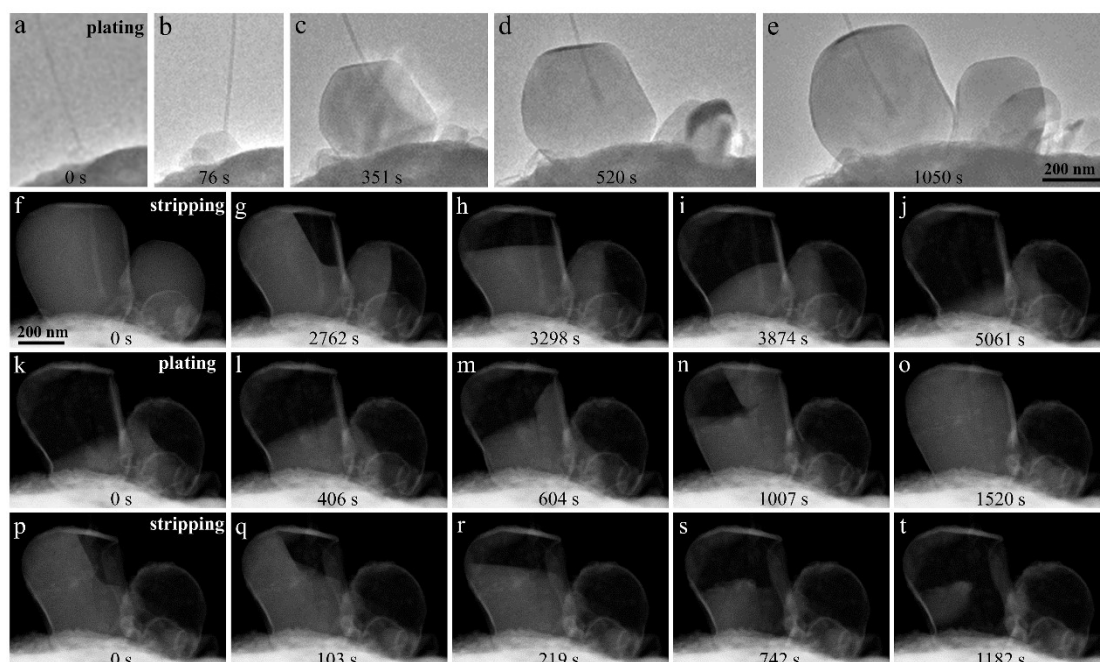


Fig. S13 Time lapse ADF images showing two cycles of Na plating/stripping. (a-e) The 1st plating process. (f-j) The 1st stripping process. Na was extracted out leaving a Na₂CO₃ shell. (k-o) The 2nd plating process. During this process, Na metal was deposited in the empty Na₂CO₃ shell. (p-t) The 2nd stripping process. Na was extracted out again with a Na₂CO₃ shell residue.

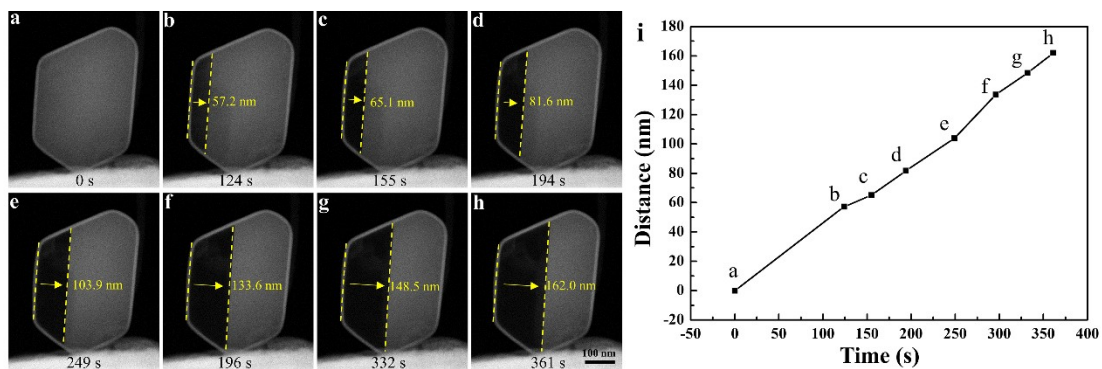


Fig. S14 Measurement of the stripping distance vs time relationship. (a-h) Time lapse ADF images of Na stripping process with sharp stripping front, whose traveling distance is marked (yellow arrows). (i) The relationship between stripping distance and time corresponding to (a-h).

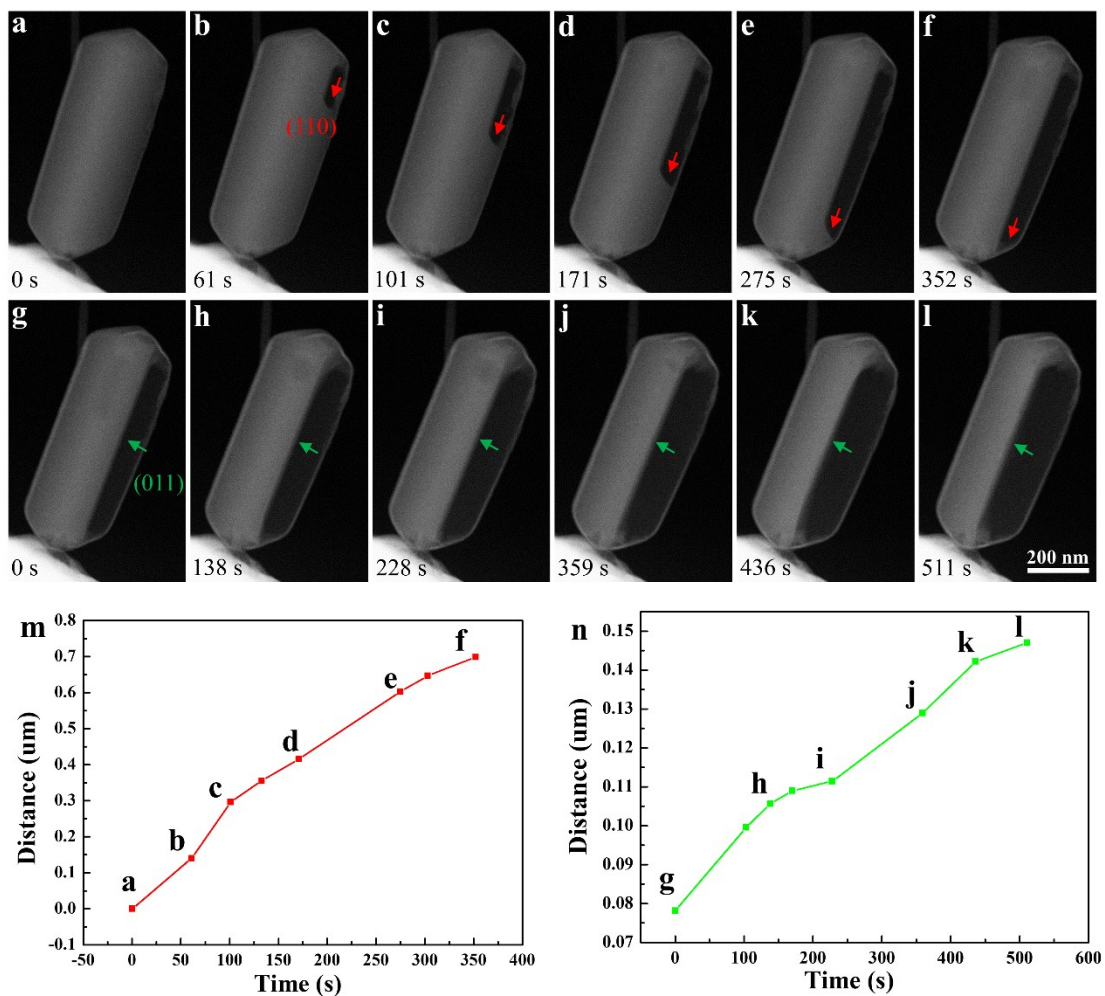


Fig. S15 Measurement of the stripping distance vs time relationship. (a-f) ADF images of Na stripping along a (110) plane. (g-l) ADF images of Na stripping along a (011) plane. (m, n) Stripping front migration distance vs time plots of two different stripping fronts shown in (a-f) and (g-l), respectively.

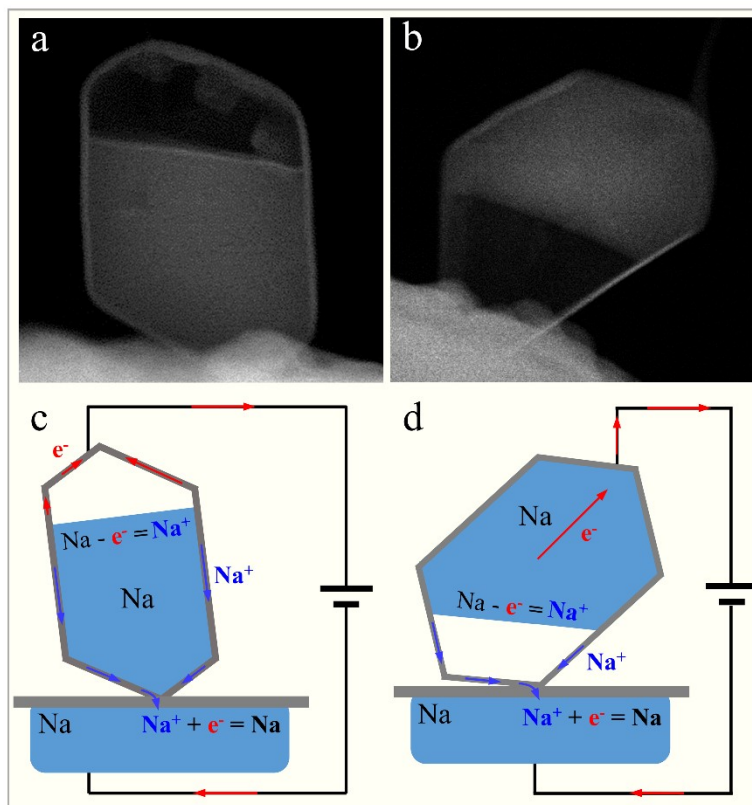


Fig. S16 Schematic of Na^+ (blue arrows) and electron (e^-) transport paths during stripping of two different residual Na polyhedral. (a) An ADF image showing that more than half Na remained in the bottom interior section of the polyhedron. (b) An ADF image showing some residual Na in the top interior section of the polyhedron. (c, d) Schematic of Na^+ (blue arrows) and e^- (red arrows) transport paths during stripping corresponding to (a) and (b), respectively.

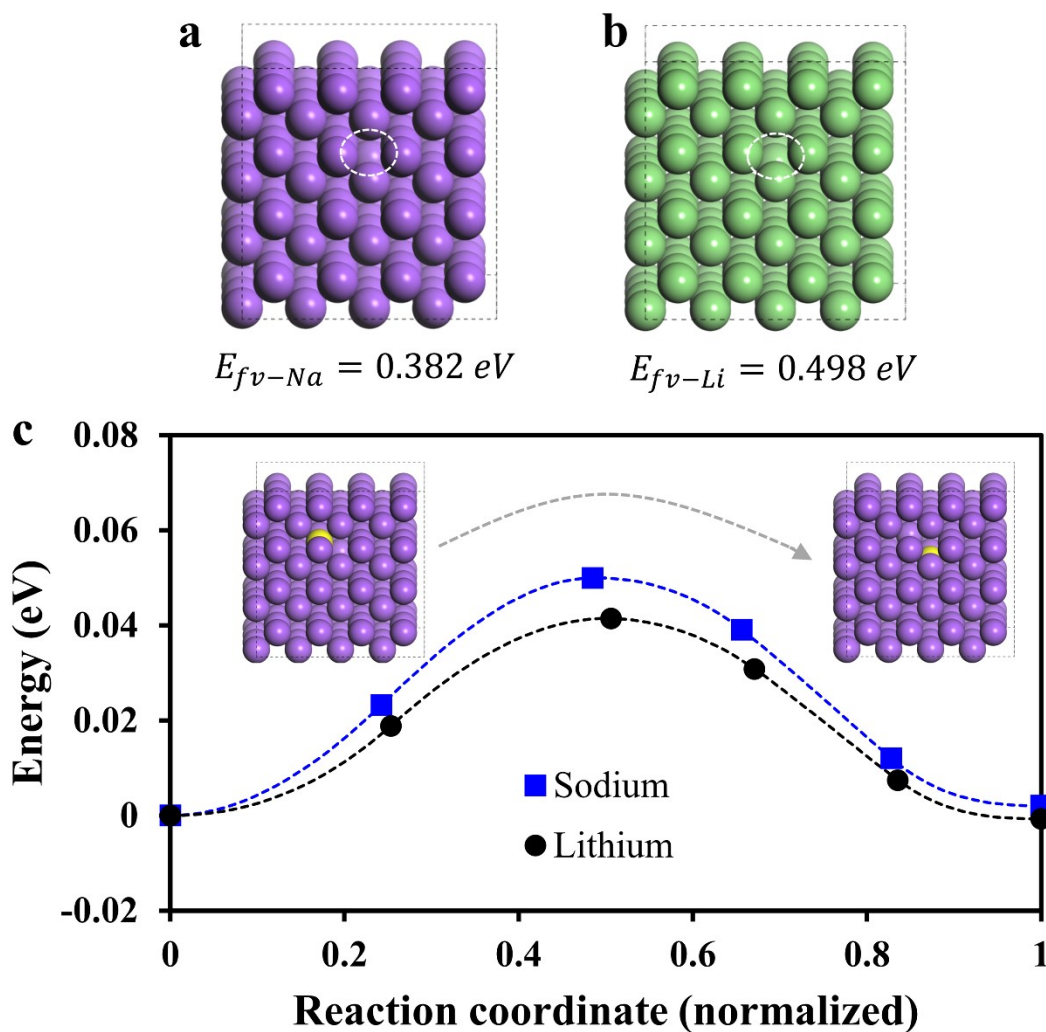


Fig. S17 Calculations of vacancy formation energies and vacancy diffusion barriers in bulk Na and Li. (a-b) Atomic structures of Na and Li with a single vacancy, in which the white dashed circles are the positions of the removed atoms. (c) The minimum energy path of single vacancy diffusion in bulk Na and Li was calculated by the nudged elastic band method by using VASP. The insets show the initial and final atomic structures during the vacancy migration path.

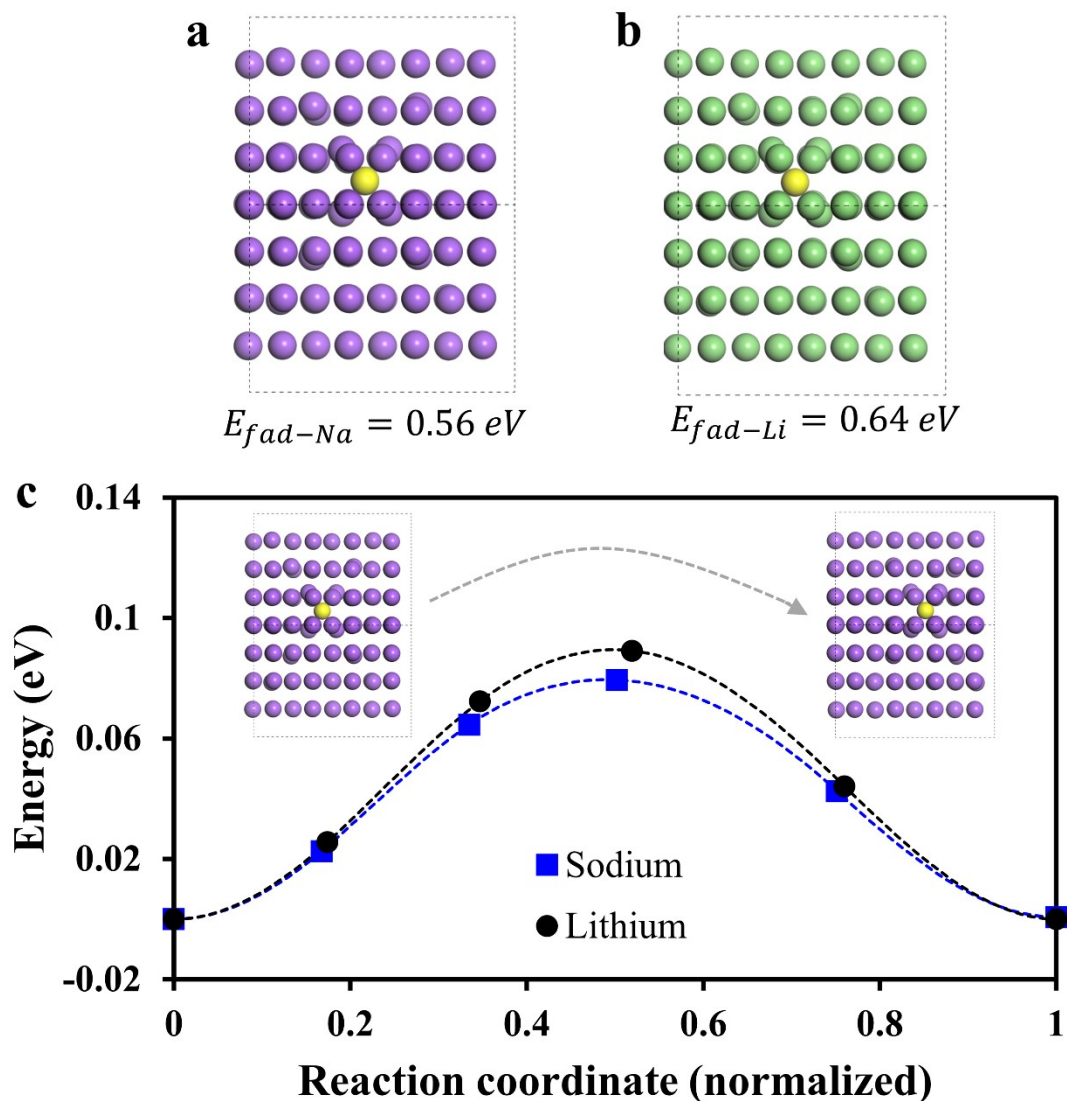


Fig. S18 Calculations of adatom formation energies and adatom diffusion barriers in bulk Na and Li. (a-b) Atomic structures of Na and Li with adatoms in yellow color. (c) The minimum energy path of single adatom diffusion in bulk Na and Li was calculated by the nudged elastic band method by using VASP. The insets show the initial and final atomic structures during the adatom migration path.

Table S1. The formation energies of Na ($10\bar{1}$) and Na ($1\bar{1}\bar{2}$) planes at different α during the stripping process.

Formation energy of ($10\bar{1}$) (eV)		Formation energy of ($1\bar{1}\bar{2}$) (eV)			
<i>Atom number</i>		<i>Atom number</i>	$\alpha=1.0$	$\alpha=1.144$	$\alpha=1.326$
1146	53.1531	1241	48.4079	55.3787	64.1744
1905	62.8428	1641	54.9378	62.8488	72.8310
2788	72.5354	2087	60.7208	69.4646	80.4976
3276	77.3828	2579	63.6581	72.8249	84.3915
3795	82.2305	3105	67.1580	76.8288	89.0314
4345	87.0787	3650	70.6581	80.8314	93.6697
4926	87.0788	4210	72.8933	83.3900	96.6347
8412	87.0762	4781	74.0132	84.6711	98.1192
11898	87.0761	5359	74.5724	85.3108	98.8606
15384	87.0770	5940	75.2232	86.0553	99.7234
		9426	75.2255	86.0579	99.7264
		12912	75.2260	86.0586	99.7271